THE JOURNAL OF PHYSICAL CHEMISTRY B

Article

pubs.acs.org/JPCB

Carbon Monoxide Recombination Dynamics in Truncated Hemoglobins Studied with Visible-Pump MidIR-Probe Spectroscopy

Andrea Lapini,[¶,†] Mariangela Di Donato,[¶,†,‡] Barbara Patrizi,[†] Agnese Marcelli,[†] Manuela Lima,[†] Roberto Righini,[†] Paolo Foggi,[†,‡,§] Natascia Sciamanna,[⊥] and Alberto Boffi[⊥]

[†]LENS (European Laboratory for Nonlinear Spectroscopy) via N. Carrara 1, 50019 Sesto Fiorentino (FI), Italy

[‡]INO (Istituto Nazionale di Ottica), Largo Fermi 6, 50125 Firenze, Italy

[§]Dipartimento di Chimica, Università di Perugia, via Elce di Sotto 8, 06123 Perugia, Italy

[⊥]Istituto Pasteur, Fondazione Cenci Bolognetti c/o Dipartimento di Scienze Biochimiche, Università "La Sapienza", piazzale Aldo Moro 5, 00185 Roma, Italy

Supporting Information

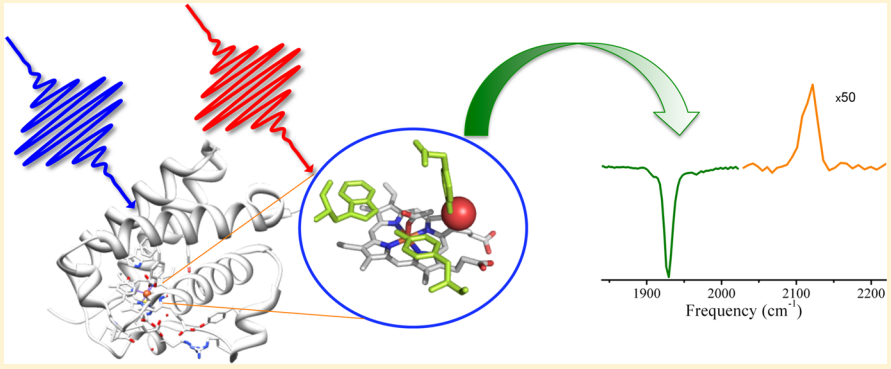

ABSTRACT: Carbon monoxide recombination dynamics upon photodissociation with visible light has been characterized by means of ultrafast visible-pump/MidIR probe spectroscopy for the truncated hemoglobins from *Thermobifida fusca* and *Bacillus subtilis*. Photodissociation has been induced by exciting the sample at two different wavelengths: 400 nm, corresponding to the heme absorption in the B-band, and 550 nm, in the Q-bands. The bleached iron−CO coordination band located at 1850−1950 cm^{-1} and the free CO absorption band in the region 2050−2200 cm^{-1} have been observed by probe pulses tuned in the appropriate infrared region. The kinetic traces measured at 1850−1950 cm^{-1} reveal multiexponential subnanosecond dynamics that have been interpreted as arising from fast geminate recombination of the photolyzed CO. A compared analysis of the crystal structure of the two proteins reveals a similar structure of their distal heme pocket, which contains conserved polar and aromatic amino acid residues closely interacting with the iron ligand. Although fast geminate recombination is observed in both proteins, several kinetic differences can be evidenced, which can be interpreted in terms of a different structural flexibility of the corresponding heme distal pockets. The analysis of the free CO band-shape and of its dynamic evolution brings out novel features about the nature of the docking site inside the protein cavity.

INTRODUCTION

Truncated hemoglobins (trHbs) are a family of small oxygen binding proteins widely distributed among bacteria, plants, and protozoa.[1,2] They are characterized by a high structural variability of the heme pocket residues, suggesting diverse functions, possibly related to the physiological response in the defense from oxygen reactive species and in the presence of other bimolecular ligands such as NO or CO. On the basis of the nature of the amino acid residues in key topological positions within the distal heme pocket, trHbs are usually divided into three groups, each presenting a certain number of conserved residues. Truncated hemoglobins from *Thermobifida fusca* (Tf-trHb) and *Bacillus subtilis* (Bs-trHb) both belong to group II, which is characterized by the presence of a Trp residue on the bottom of the heme distal pocket (G8 position).[1] The resolution of the crystal structure of a number of group II truncated hemoglobins has revealed a common general pattern of the heme pocket, characterized by an ensemble of polar residues capable of forming hydrogen bonds with the iron-bound ligand, usually defined as "ligand inclusive hydrogen bonding network" (see Figure 1). It has been suggested that TrpG8 plays an important role in ligand binding and stabilization, though other amino acids in topological positions E7, E11, CD1, and B10 can modify drastically the

Received: February 27, 2012
Revised: June 22, 2012
Published: July 3, 2012

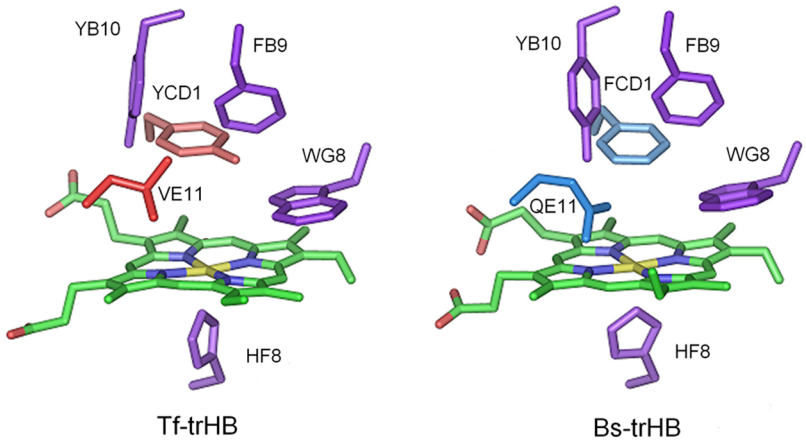

Figure 1. Close-up view of the active sites in *Thermobifida fusca* and Bacillus substilis truncated hemoglobins. The key topological positions in contact with the iron bound ligand (E11, B9, B10, CD1, and G8) are shown for both proteins. Conserved residues in both proteins are colored magenta. Nonconserved amino acids are in red (Tf-trHb) or in cyan (Bs-trHb). Pictures generated with PyMol (DeLano Scientific LLC).

interaction network.[3−5] The structure and sequence analysis of group II trHbs shows that the nature of the residue at position CD1 is correlated with the nature of the site E11. When the protein has a Tyr at CD1, a nonpolar residue is found at E11; in contrast, when a non-hydrogen bond donor replaces the TyrCD1, a hydrogen bond donor is present at the E11 site. TyrB10 and TrpG8 are instead invariant residues.[6,7] The crystal structure of both Tf-trHb[8] and Bs-trHb[9] has been resolved, confirming a high degree of similarity among these two proteins. In the case of Tf-trHb, the heme distal pocket involves, beside TrpG8, two Tyr residues, TyrB10 and TyrCD1, which are in close proximity with the iron-bound ligand. In Bs-trHb, the more closely ligand interacting residues besides TrpG8 are TyrB10 and GlnE11.

Given the high sensitivity of the ν(CO) stretching vibration of the hemoglobin-CO adduct to the electric field generated by the protein environment, Resonance Raman and FTIR spectra have been used to probe the local structural characteristics of the heme binding pocket for the heme-bound CO state of both Tf-trHb and Bs-trHb. It has been found that each of these two proteins can adopt two different conformations, differing by the number of hydrogen bonds formed with the iron-coordinated CO.[3,10,11]

In the case of Tf-trHb, the comparison of the FTIR spectra of the wild type protein and of a series of combinatorial mutants in which TrpG8, TyrCD1, and TyrB10 have been changed into Phe, revealed that in one conformation both TrpG8 and TyrCD1 are hydrogen bonded to the iron-coordinated CO, while in the other conformer only the H-bond with TrpG8 is maintained. The FTIR spectrum of the CO adduct of the wild type protein showed two bands attributable to the ν(CO) stretching vibration, located at 1920 and 1940 cm^{-1}, respectively. These features have been ascribed to the presence of two conformers in which the iron coordinated CO is either doubly H-bonded to both TrpG8 and TyrCD1 or singly bonded only to TrpG8, respectively.[10]

Very similar structural characteristics are observed also for Bs-trHb. In the latter protein, the FTIR spectrum of the CO adduct also shows two bands assigned to the ν(CO) stretching vibration: one extremely downshifted, at 1888 cm^{-1}, and the other at 1925 cm^{-1}. The spectra have been interpreted along the same line as in Tf-trHb, that is, by assuming the presence of a doubly H-bonded species in which TrpG8 and TyrB10 are hydrogen bonded to the iron coordinated CO, and a singly H-bonded adduct in which TrpG8 is the sole H-bonding residue. The extreme downshift of the ν(CO) stretching vibration at 1888 cm^{-1} indicated a highly polar environment around the bound CO, in which the double H-bond dominates the ligand dissociation and rebinding dynamics properties of Bs-trHb.[3] The sizably lower frequency of the ν(CO) stretching band in Bs-trHb, as compared to Tf-trHb, can be a consequence of a more favorable orientation of the coordinating residues toward the ligand. Such sterically favorable conformation is suggested to generate a stronger H-bonding interaction and consequently a higher degree of electron back-donation toward the iron. This finding may account for the 1 order of magnitude higher oxygen affinity in Bs-trHb with respect to Tf-trHb despite the similar structural characteristics of the distal heme pockets in the two proteins.[3]

The structural features of the heme distal pocket are known to govern the dynamics of ligand escape and recombination in globins. Recombination dynamics can vary substantially, spanning from the millisecond time scale of myoglobin and hemoglobin[12,13] to the subnanosecond time scale observed for instance in the oxygen sensory protein FixL.[14,15] In Bs-trHb CO recombination dynamics has been studied by transient visible absorption spectroscopy, revealing the existence of a very fast geminate recombination dynamics with a time constant of about 770 ps.[3] The occurrence of fast geminate recombination suggests that the ligand is confined within the distal pocket with little possibility for the CO molecule to escape from the protein matrix to the solvent.

To capture further details on the way such proteins operate we analyzed the CO escape and rebinding processes after dissociation induced by a short laser pulse by applying visible-pump MidIR-probe spectroscopy in both Bs-trHb and Tf-trHb. The combination of the high temporal resolution given by short laser pulses with the structural information achieved by the infrared probe, provides unique pieces of information on the microscopic environments experienced by the ligand molecule after photodetachment, unattainable by UV−vis probe pulses. This technique has been widely applied in the past to study carbon monoxide recombination dynamics in a number of similar systems, such as myoglobin, hemoglobin, and the oxygen sensory protein FixL.[13−19] In the present study, the comparison between two proteins investigated in further details

dx.doi.org/10.1021/jp3019149 | J. Phys. Chem. B 2012, 116, 8753−8761

provides insight on the factors influencing the amount and the dynamics of geminate recombination and on the microscopic environment determining the impaired escape of the ligand after photolysis.

MATERIAL AND METHODS

Protein Expression and Purification-Sample Preparation. *Bacillus subtilis* and *Thermobifida fusca* hemoglobins were obtained and purified as described previously.[8,9] In addition, Tf-trHb was successfully obtained as a lyophilized sample.

Protein solution for vis-pump MidIR-probe measurements were prepared by dissolving the samples in a Tris-HCl buffer, 0.2 M, in D_2O (pD = 8). In the case of Tf-trHb, a 10 mM solution was prepared by dissolving a lyophilized protein preparation in the buffer, while for Bs-trHb, solutions at 4 mM concentration were obtained by microcentrifugation with Millipore ultracon filters. The reduction of proteins was accomplished by adding a freshly prepared anaerobic solution of sodium dithionite in stoichiometric excess to the protein solution, previously degassed with nitrogen. Carbon monoxide (Rivoira), was gurgled at low flux intensity, and the sealed protein solution was saturated with 1 atm CO for 15 min. In this way CO is homogeneously distributed despite the high viscosity of the sample. Samples for transient infrared measurements were prepared by squeezing about 40 μL of solution between two calcium fluoride windows (3 mm thickness) separated by a 50 μm Teflon spacer (in the case of Bs-trHb, a 100 μm spacer was used). The OD at the excitation wavelength was about 0.8 for all samples.

Visible-Pump/MidIR-Probe Spectroscopy. Measurements were performed probing both the absorption region of the ν(CO) stretching vibration of the iron-bound CO (1880−1990 cm^{-1} for Tf-trHb and 1825−1975 for Bs-trHb) and the dissociated free CO absorption (2030−2230 cm^{-1}). CO dissociation was induced by pumping the systems either with a 400 or a 550 nm laser pulse. The experimental setup for the infrared differential absorption measurements has been described in detail in ref 20. Briefly, a Ti:sapphire oscillator/regenerative amplifier, operating at 1 kHz, (Legend, Coherent) was used to pump a home-built optical parametric generator and amplifier with difference frequency generation, which produced a tunable output (2.5−10 μm) with a spectral width of ∼200 cm^{-1}. The output of a HgCdTe camera system, placed behind a spectrograph, was read out every shot at a repetition rate of 1 kHz and a sampling resolution either of 3 or 6 cm^{-1}. In case of the blue excitation, another part of the Legend output was frequency doubled in a BBO crystal to generate the pump-pulses at 400 nm (∼6 nm fwhm) which were attenuated to provide 200−500 nJ and focused to a spot of ∼150 μm in diameter. Excitation pulses at 550 nm (energy = 200 nJ) were obtained by sum frequency generation of the idler output of a commercial optical parametric generator (TOPAS, Light Conversion) with a portion of the fundamental output at 800 nm. A moveable delay line made it possible to increase the time-of-arrival-difference of the pump and probe beams up to 1.8 ns. The pump beam polarization was set to magic angle with respect to the probe beam by rotating a $\lambda/2$ plate. Furthermore anisotropy measurements were executed by setting the pump beam polarization either at 0 or 90 degrees with respect to the probe beam. The sample was moved with a home-built scanner to refresh the solution and avoid photodegradation. Home-written software was used to collect the data over the two different spectral windows, respectively, between 1880 and 1975 cm^{-1} and 2030−2230 cm^{-1}. Every window was recorded with a freshly prepared sample and measured at least three times. To obtain a good signal-to-noise ratio in the case of the free CO signal, which has a small absorption cross section, a number of data sets, corresponding to about 12000 laser shots were collected and averaged. The integrity of the sample has been checked by FTIR (Bruker Alpha-T) and visible absorption (Perkin-Elmer LAMBDA 950) before and after the time-resolved measurements.

Data Analysis. For the quantitative analysis of the time-resolved spectral data we used a combined approach, consisting of singular values decomposition (SVD) and the simultaneous fitting of all the collected kinetic traces (global analysis). To avoid the contribution due to perturbed free induction decay and cross-phase modulation,[21−25] we excluded from our analysis the spectra measured for delays shorter than 500 fs. First, we extrapolated the number of components using SVD;[26−28] then we analyzed the whole ensemble of kinetic data by means of a global fitting procedure. The combination of global analysis and SVD is a very helpful analysis protocol, as it provides a good control on the number of components used to fit the data.[29−34] The time constants resulting from the fitting of the right singular vectors were used as the starting point for the subsequent global analysis. The aim of global analysis is to decompose the two-way data matrix into time-independent spectra and wavelength-independent kinetics.[33−36] Once the number of components has been identified, the second step involves the parametrization of the time evolution of the relative intensities of the spectral components. This was accomplished by assuming a first-order kinetics, describing the overall temporal evolution as the sum or combination of exponential functions. Global analysis was performed using the GLOTARAN package (http://glotaran.org).[34,37−40] We employed a linear unidirectional "sequential" model. The solution for the system of differential equations for the "sequential" model with increasing lifetimes is

$$c_l(t) = \sum_{j=1}^{l} b_{jl} \exp(-k_j t)$$

$$b_{jl} = \prod_{m=1}^{l-1} k_m / \prod_{\substack{n=1 \\ n \neq j}}^{l} (k_n - k_j)$$

$c_l(t)$ represent the temporal evolution of the selected component, k_j is the decay rate of component j and the amplitudes b_{jl} of the exponential decays are defined for $j \leq l$ assuming $b_{11} = 1$. In discussion of our results the spectra associated to the various time constants are termed "evolution associated difference spectra" (EADS).

RESULTS

Thermobifida fusca. Initial experiments on Tf-trHb were performed by exciting the sample with a 400 nm pump pulse, whose energy was varied between 200 and 500 nJ. The spectrum recorded immediately after excitation shows the appearance of a bleaching signal in the spectral region where the ν(CO) stretching vibration is expected, indicating photolysis of the ligand. A main bleaching band and a small shoulder are visible, respectively peaking at 1920 and 1940 cm^{-1}, in good correspondence with the absorption bands measured in the FTIR spectrum of the CO adduct for this protein, see Figure 2a. Experiments were repeated by setting

dx.doi.org/10.1021/jp3019149 | J. Phys. Chem. B 2012, 116, 8753−8761

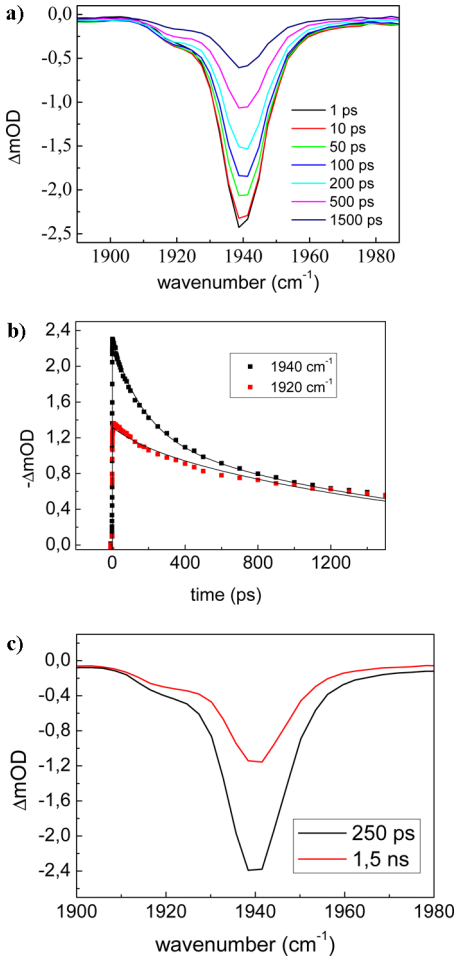

Figure 2. (a) Time resolved spectra recorded at different time delays, showing the bleaching induced by the excitation at 400 nm in the ν(CO) stretching region for the coordinated CO; (b) Kinetic traces (scattered points) at selected frequencies together with the fit (solid line) obtained by global analysis. The trace at 1920 cm^{-1} has been scaled to overlap the trace at 1940 trace on the long time scale; (c) EADS obtained by globally analyzing all the kinetic traces recorded in the 1850−1950 cm^{-1} spectral range.

the pump pulse polarization either to 0 or 90 degrees with respect to the probe pulse, and the time-dependent anisotropy of the transition was calculated, resulting in an average value of −0.18. Considering that the heme behaves like a circular absorber when excited at 400 nm,[41,42] it can be calculated that the coordinated CO is oriented in way that its dipole forms an angle smaller than 15 degrees with respect to the heme normal, similarly to what observed for other globin proteins.[14,17,43]

The analysis of the kinetic traces revealed a biphasic recovery, occurring within the subnanosecond time scale. As clearly visible by inspecting the kinetic traces reported in Figure 2b, the bleaching band at 1940 cm^{-1} recovers faster than the bleaching at 1920 cm^{-1}. We have analyzed the data using a global fit with a sequential decay scheme, obtaining the EADS reported in Figure 2c. The kinetic traces can be satisfactorily fitted with two components, whose time constants are 250 ps and 1.5 ns, respectively. The fast kinetic phase accounts for almost 30% of the recombination dynamics at 1940 cm^{-1}. An inspection of the kinetic traces reported in Figure 2b brings out that the relative weight of the fast component is much higher for the 1940 cm^{-1} band with respect to the low frequency band (1920 cm^{-1}).

Bleaching recovery on a subnanosecond time scale can be directly associated to fast geminate recombination if it is assumed that the recombined CO and CO in the non-photolyzed portion of the sample have the same spectrum as the ligated CO at equilibrium.[43] To further investigate the dynamics following CO photodissociation we also analyzed the free CO absorption band, which is expected to appear at about 2100−2150 cm^{-1}. Because of the low absorption cross section of the free CO vibration and the substantial water absorption in that region, it is difficult to obtain reliable kinetic traces and time-dependent spectra with a good signal to-noise-ratio. Tentative measurements, carried out by exciting the sample with a 400 nm pump pulse, revealed a significant baseline problem, due to water absorption, heating, and excess energy dissipation in the system. To minimize these unwanted contributions, CO photolysis was triggered by exciting the heme in the Q-band absorption region (550−600 nm) instead of the B-band region. Under these experimental conditions the amount of energy dissipated by the system was significantly reduced.

Measurements were thus carried out by setting the excitation pulse at 550 nm and probing both the ν(CO) stretching region for the coordinated CO and the free CO absorption region. The dynamic evolution in the bleaching region was substantially identical to what was previously observed by exciting the sample at 400 nm. Instead, significant improvement was obtained in the free CO region, were time traces with good signal-to-noise ratio could be recorded.

Spectra collected in the free CO region are reported in Figure 3a while Figure 3b shows the kinetic trace measured at the absorption maximum and compared with that of the 1940 cm^{-1} bleaching band, which has been scaled to match the

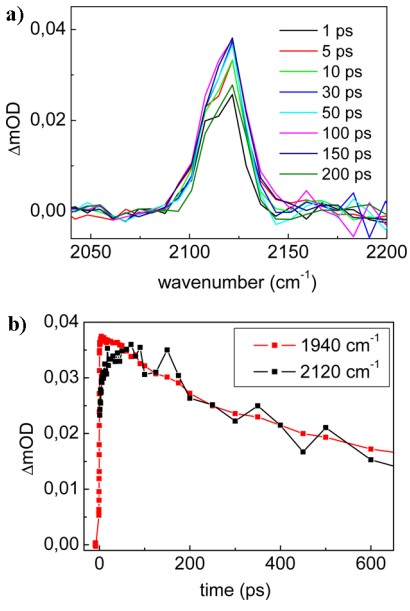

Figure 3. (a) Time resolved spectra in the free CO region recorded at different time delays after excitation of the sample with a 550 nm laser pulse; (b) kinetic traces at 2120 cm^{-1} (red line), corresponding to the maximum absorption in the free CO region. This trace has been superimposed with the kinetic trace at 1940 cm^{-1} (black line), corresponding to the maximum absorption of the coordinated CO, opportunely scaled.

dx.doi.org/10.1021/jp3019149 | J. Phys. Chem. B 2012, 116, 8753−8761

intensity of the free CO signal. As noticed from Figure 3b, the two kinetic traces are well matched, except for the short time scale, where the signal corresponding to the CO absorption (2120 cm^{-1}) shows an initial rise component.

Spectra in Figure 3a have been corrected for the presence of a baseline, which still contributes in this region although at a more minor extent than in the previous measurements with 400 nm excitation. The baseline is removed by subtracting a third order polynomial fit (initial raw data and baseline subtracted are shown in Supporting Information). To avoid the influence of the baseline correction procedure on the dynamic behavior of the system, the region between 2080 and 2150 cm^{-1}, where the signal is observed, was removed for the fit. Our data show a ratio in the absorption cross section between the coordinated and docked CO of about 50, in agreement with previous findings.[43] Baseline problems are less significant in the bleaching region, which is free from water absorption. In this region, the amplitude of background fluctuation has a negligible influence on the kinetics (see Supporting Information for details).

As reported in Figure 3b, the dynamic evolution in the free CO absorption region matches that of the 1940 cm^{-1} bleaching, thus confirming that also the fast 250 ps component has to be ascribed to geminate recombination. At the early measured times a rise of the free CO absorption signal is observed, which can be fitted with a time constant of 30 ps. An initial rise component for a docked CO band has been previously observed also for myoglobin[17] and interpreted in terms of protein relaxation around the photolyzed CO molecule. In that case however the rise component had a much faster time constant of about 1.6 ps. Furthermore thermal relaxation has also been observed to occur for myoglobin excited at 597 nm, with a time constant of 6.2 ps.[44] The longer time scale observed in this case for the rise component may indicate a combination of slower cooling process and/or a more significant protein rearrangement, possibly involving the rotation or reorientation of one or more amino acid side chains in the CO docking site. Such structural adjustment most likely modifies the electrostatic interactions around the CO molecule thus increasing the oscillator strength.[45] This is probably the consequence of a more flexible heme pocket structure, also brought out by the presence of a water molecule, which could rearrange by breaking/forming H-bonds with the tyrosine amino acids (TyrB10 and TyrCD1) located at a short distance from the heme.

Besides the 30 ps component, a global fit of the kinetic traces collected in the free CO region (2050−2200 cm^{-1}) results in two additional decay components, with time constants of 300 ps and 1.2 ns, respectively. These time constants qualitatively agree with those measured for the bleaching recovery, thus confirming that the process responsible for the dynamic evolution of the system is a fast geminate recombination of the photolized CO. The EADS obtained by globally analyzing the kinetic traces in the 2050−2150 cm^{-1} region with a sequential decay scheme are reported in the Supporting Information. To take into account of the bandwidth variation with time, we estimated the temporal evolution of the integrated area of the CO band, and we compared it with the kinetic trace at 2120 cm^{-1}, corresponding to band maximum. The two traces are qualitatively in good agreement (see Supporting Information).

The measured CO absorption peak is quite asymmetrical and has a rather large bandwidth (fwhm 30 cm^{-1}), which suggests the presence of an inhomogeneous distribution of two unresolved bands behind the measured line shape. The signal dynamically evolves by slightly shifting to the blue, but no substantial line shape variations are observed. Although it has been shown that in similar systems a certain percentage (reported values span between 3.6 and 13%) of the photolized CO is initially in a vibrationally hot state[13,14,17,19,46,47] no vibrational hot band could be resolved in the present case. Since the CO anharmonicity has been estimated to be 27−30 cm^{-1}[13,47] hot bands are probably not resolved due to baseline fluctuation problems.

Bacillus subtilis. Also in the case of Bs-trHb, time-resolved spectra in the bleaching region were collected by exciting the sample both with a 400 nm and a 550 nm laser pulse. Again, no significant differences were observed in the dynamic evolution of the system between the two excitation wavelengths. Following CO photodissociation, two bleaching bands are observed at 1925 cm^{-1} and 1888 cm^{-1}, respectively, whose positions well correspond with the measured FTIR spectrum of the CO adduct for this protein, see Figure 4a. The

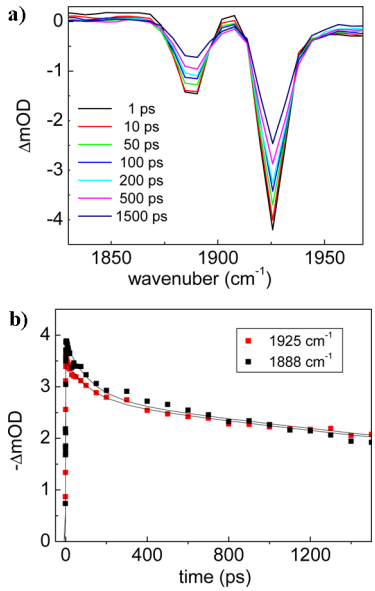

Figure 4. (a) Time resolved spectra recorded at different time delays, showing the bleaching induced in Bs-trHb in the ν(CO) stretching region for the coordinated CO. Excitation wavelength was 550 nm. (b) Kinetic traces (scattered points) together with the fit (solid line) obtained by global analysis at selected frequencies, corresponding to the two maximum absorptions in the iron coordinated CO region. The trace at 1888 cm^{-1} has been scaled to overlap the trace at 1925 cm^{-1}.

corresponding kinetic traces, reported in Figure 4b can be fitted with two time constants of 120 ps and 2 ns, respectively. In contrast to what was observed in Tf-trHb, the two bleaching bands in Bs-trHb recover with the same kinetics. In this case the faster kinetic component has a very low weight, only accounting for less than 10% of the recombination dynamics for both bleaching bands, implying that the fraction of picosecond geminate recombination is lower than that observed in Tf-tbHb. Fast geminate recombination in Bs-trHb has been previously observed through time-resolved measurements in the visible spectral range.[3] In the present infrared measurements a 30 ps component, previously identified by transient absorption measurements in the visible region, is not observed. Since the currently probed spectral range is only sensitive to

dx.doi.org/10.1021/jp3019149 | J. Phys. Chem. B 2012, 116, 8753−8761

CO vibrations, we conclude that this 30 ps component is not associated to fast ligand recombination, but probably represents a relaxation process of the heme.

The free CO region was probed by exciting the sample at 550 nm. The time-resolved spectra in this region are qualitatively similar for both proteins, but striking differences are observed in their kinetics. Also for Bs-trHb only one band is observed, whose dynamic evolution follows that of the bleaching signals, though with minor intensity. The peak shape of the docked CO is not completely symmetrical and the fwhm is about 30 cm^{-1}. Time resolved spectra of the free CO in Bs-trHb, shown in Figure 5a, show a blue shift on a 10 ps

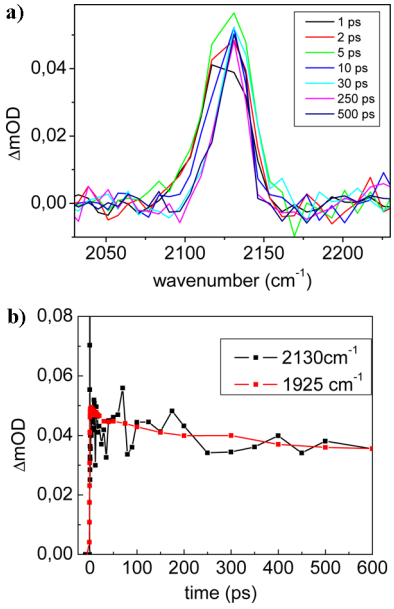

Figure 5. (a) Time resolved spectra in the free CO region recorded at different time delays after excitation of the sample with a 550 nm laser pulse; (b) Kinetic traces at 2130 cm^{-1} (black line), corresponding to the maximum absorption in the free CO region in Bs-TrHb. The trace has been superimposed with the kinetic trace at 1925 cm^{-1} (red line), corresponding to the maximum absorption of the coordinated CO.

time scale, which could be an indication for vibrational cooling. Alternatively there could be two bands hidden under the observed line shape, with a population exchange occurring on this time scale. Given the low signal-to-noise ratio of the measurements, these observations have to be considered with care, and in order to better rationalize this spectral evolution, measurements should be repeated with a higher spectral resolution.

The kinetic trace for the maximum of the absorption band, compared with that of the scaled bleaching trace measured at 1925 cm^{-1} is reported in Figure 5b. In Figure 6, the kinetic traces corresponding to the maximum absorption of the free CO band are compared for the two analyzed proteins. The observed signals bring out clearly a more intense slow phase and a faster decay in the case of Tf-trHb with respect to Bs-trHb.

DISCUSSION

The possibility to follow CO recombination dynamics in the infrared spectral window, after photolysis induced by a short laser pulse, provides unique information about the influence of structural and electrostatic properties of the distal heme pocket

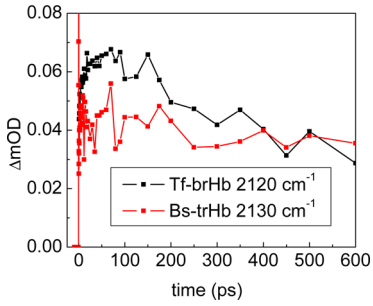

Figure 6. Kinetic trace at 2120 cm^{-1} recorded at the maximum absorption in the free CO region in Tr-trHb (black line) compared with the corresponding kinetic trace measured in Bs-trHb at 2130 cm^{-1} (red line).

on the ligand dissociation and rebinding processes occurring in globin proteins. While pump−probe measurements in the visible spectral range give only indirect information on the recombination dynamics, since they can only probe the evolution in the electronic state of the heme moiety after excitation, measurements in the infrared are much more specific, since they can probe the dynamics of the vibrational bands of the ligand before and after photolysis, thus providing a direct snapshot of the transient state of the photolyzed CO molecule. In this work we have shown that, in the case of Bs-tbHb, the infrared probe has allowed the unambiguous assignment of a 30 ps component previously identified by visible transient absorption measurements.[3] The absence of this kinetic component in the current measurements within the infrared spectral range, leads to the conclusion that it is not associated to fast ligand recombination, but most likely represents a relaxation process of the heme.

Furthermore, important information on the influence of the distal pocket structure on the recombination dynamics can be retrieved with this technique. In this study we have compared two truncated hemoglobins, *Thermobifida fusca* and *Bacillus subtilis,* whose distal heme pockets, shown in Figure 1, are at a first sight very similar.

Despite the structural similarities in the architecture of the heme pocket, Tf-trHb and Bs-trHb display significant differences in the dynamics of ligand exchange and rebinding. Present results indicate that although both proteins show fast geminate recombination, the relative amount of the picosecond dynamic phase is not the same. To highlight these differences we have compared in Figure 7a and 7b the kinetic traces measured for the two bleaching bands of Tf-trHb (1940 and 1920 cm^{-1}) with the corresponding bands observed for Bs-trHb (1925 and 1988 cm^{-1}).

For both proteins two different conformations have been identified on the basis of FTIR measurements, herein referred as an "open" conformation, characterized by a single amino acid H-bonded to the ligand and a "closed" conformation, characterized as having two H-bonded residues.[3,10]

In the case of Tf-trHb, the dynamics of bleaching recovery of the open and closed conformations are different. The open conformation, responsible for the infrared band at 1940 cm^{-1} substantially recovers with a fast 250 ps component, while for the closed one, the picosecond component only accounts for a minor fraction of signal recovery.

It is commonly accepted in the literature that the presence of H-bonds between the residues in the distal pocket and the heme bound CO favors the occurrence of fast recombination.

dx.doi.org/10.1021/jp3019149 | J. Phys. Chem. B 2012, 116, 8753−8761

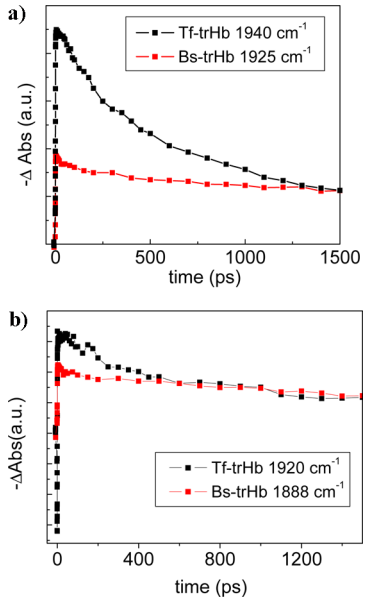

Figure 7. Comparison between the kinetic traces in the bleaching region for Tb-trHb and Bs-trHB upon excitation at 550 nm. (a) Trace at 1940 cm^{-1} of Tf-trHb (black line) compared to the trace at 1925 cm^{-1} of Bs-trHb (red line). The two kinetic traces have been scaled to overlap on the long time scale. (b) The 1920 cm^{-1} of Tf-trHb (black line) compared to the trace at 1925 cm^{-1} of Bs-trHb (red line).

For instance it was recently shown that in the oxygen sensory protein FixL, the introduction of a residue capable of forming H-bonds with the iron bound CO, through the mutation R220H, determines the occurrence of substantial contribution to geminate recombination on a 250 ps time scale.[14,48]

On that basis one would expect to observe a substantial amount of picosecond geminate recombination also in Bs-trHb, since, for this protein, the highly downshifted ν(CO) stretching measured by FTIR indicated the presence of strong H-bonds between the iron coordinated CO and the residues in the distal pocket. Nevertheless our results show that only a minor fraction of the photolized CO, corresponding to less than 10% of the total, recombines with a 120 ps kinetics. The fraction of the fast dynamic phase is the same for both the open and closed conformations of the protein, being thus independent of the number of H-bonds formed by the coordinated ligand. We also note that, in Tf-trHb, the higher fraction of fast recombination is observed in the open conformation, that is, the one with only one H-bond and not, as it would be expected at a first sight, when both TyrCD1 and TrpG8 are H-bonded to the coordinated CO. A similar behavior has been observed in the case of myoglobin, in which time-resolved infrared spectra measured at low temperature showed the appearance of two bleaching bands (at 1944 and 1926 cm^{-1}), recovering on a different time scale. Even in this case the higher frequency band, corresponding to an open configuration, recovers faster than the low frequency one, like in Tf-trHb.[42]

Therefore it appears that a simple structural analysis only accounting for the number of hydrogen bond interactions of the iron coordinated ligand is not sufficient to interpret the kinetic differences observed among different globin proteins.

By comparing the behavior of the two truncated hemoglobins here studied, it can be suggested that one of the main factors influencing the amount of fast geminate recombination is the structural flexibility of the heme pocket. The steric hindrance of the residues surrounding the ligand, which can act as a cage confining the CO in the docking site, avoids its escape toward the solvent. If the docking site of the photolyzed CO is sufficiently large, because of the presence of smaller residues in the distal pocket, the recombination is slower. On the contrary if bulky residues impair ligand escape, the CO molecule may possibly recombine with the iron atom on a faster time scale.

These observations are still not sufficient to explain the different dynamics observed for the two conformations of Tf-trHb. In this protein, the residue TyrCD1, which in the closed conformation is at H-bond distance from the iron coordinated CO, is believed to have a high structural flexibility, being alternatively capable of forming a H-bond either with a water molecule localized in its proximity or with the ligated CO. It would be expected that, when this residue is rotated toward the ligand, as in the closed conformation, it would prevent the photolyzed CO from escaping far from the heme. In the open conformation TyrCD1 is rotated away from the ligand instead, so it may allow the CO molecule to move further away from the heme upon photolysis. In contrast, in the experimental conditions used in this work, we observe a faster rebinding for the open conformation. This may indicate that the differences among the two protein conformations can involve more rearrangements than TyrCD1 rotation. One possibility is that when TyrCD1 is rotated away from the ligand, the conserved water molecule located in the distal site assumes a position such to block the CO exit. Alternatively there could be rearrangements in the position of other residues, not identified in the currently available crystal structure, acquired without coordinated CO,[8] which eventually make the open conformation even more restrained than the closed one. It thus appears that in case of this protein it is not totally correct to refer to the two conformations as open or closed, only considering the number of hydrogen bonds formed with the iron-bound CO, while it would be more appropriate to identify them as a less constraining and more constraining conformation.

For Bs-trHb we have described until now the closed conformation as the one where both TrpG8 and TyrB10 are H-bonded to the ligand, and the open conformation as the one where only the H-bond with TrpG8 is maintained. In this case there is little difference in the dynamics of CO recombination between them. Possibly, the configuration adopted by TrpG8 and the other pocket residues is not very different for the two conformations, so that the volume of the docking cavity remains always similar. Furthermore the other residue which in the distal pocket of Bs-trHb is located at a short distance from the coordinated CO is GlnE11, whose hindrance is certainly lower if compared to that of TyrB10, which in Tf-trHb is also at short distance from the CO, besides TrpG8 and TyrCD1. It is worth noting that the importance of GlnE11 in stabilizing the coordinated ligand in Bs-trHb has been recently highlighted. According to molecular dynamic simulations, GlnE11 can adopt two different conformations, forming a H-bond alternatively either with the iron-bound CO or with TyrB10.[49] By switching among these two conformations, GlnE11 would open a cavity directly connecting the heme distal pocket with the solvent, thus favoring ligand escape. This finding would explain the high oxygen affinity observed for Bs-TrHb and strengthen the suggestion that the volume of the heme cavity and its structural flexibility have a strong influences on the fraction of fast geminate recombination.[49] Compared to Tf-trHb, in this case there is less protein reorganization after

dx.doi.org/10.1021/jp3019149 | J. Phys. Chem. B 2012, 116, 8753−8761

photolysis, possibly because the docking site is already sufficiently large to accommodate the dissociated ligand, due to the topological substitution between TyrCD1 with PheCD1 and LeuE11 with GlnE11. A lower degree of protein rearrangement induced by the ligand dissociation could also explain the absence of a rise component in the kinetics of the photodissociated CO.

Similar considerations regarding the caging effect[50,51] played by the amino-acid residues surrounding the photolyzed CO can also be applied to other recently studied systems. Picosecond geminate recombination has also been found in the CO complex of nonglobin proteins, such as microperoxidase and in the chemically modified form of cytochrome *c*, termed carboxymethyl cytochrome *c*.[52] In the former system a time constant of 110 ps has been estimated for concentrated samples,[53] while in the latter system a multiphasic recombination with time constant of 16 ps, 120 ps, and 1 ns has been measured.[54] The authors attributed the three phases to CO rebinding from different locations within the distal pocket site. The high efficiency of the ligand rebinding has been interpreted even in this case as a consequence of a sterically hindered and "caged" nature of the distal heme pocket, from which it is difficult for the ligand to escape. In these systems, the short time scale of the geminate rebinding has been correlated to a protein configuration that assures the restraint of the reorganization energy of the active site.[54]

As a final comment, it should be pointed out that the kinetic analysis presented until now does not take into account that a fraction of the photolyzed CO escapes to the solvent, and recombines on a much slower time scale with a bimolecular process. A direct estimation of the relative amount of geminate and bimolecular recombination would require following the system dynamics on a time scale spanning from picoseconds to milliseconds, which is not feasible with the currently used experimental set up. However, it is possible to have an estimate of the amount of geminate recombination occurring on the picoseconds time scale by evaluating the ratio between the areas of the EADS obtained by global analysis. In the case of Tf-trHb it can be estimated that about 40% of CO undergoes picosecond geminate recombination. The evaluation of kinetic component in the nanosecond regime is affected by a large (~20%) indetermination due to the lack of data regarding the bimolecular recombination.

CONCLUSIONS

Time resolved vibrational spectroscopy, employed to study carbon monoxide photodissociation and rebinding in two truncated hemoglobins, has revealed key structural and dynamic properties of the ligand binding process in these unusual globins. The results of this study highlight striking differences between the dynamics of CO recombination in the truncated hemoglobins with respect to other globins, such as vertebrate myoglobins and hemoglobins. Both the truncated hemoglobins from *Thermobifida fusca* and *Bacillus subtilis* exhibit subnanosecond multiexponential geminate recombination, which account for at least 50% of the total yield of CO recombination. Several conserved residues in the distal heme pocket of both the analyzed proteins, capable of interacting with the iron coordinated ligand through the formation of H-bonds, acts as a cage on the dissociated CO, preventing its escape toward the solvent and confining it in the heme cavity, thus favoring fast rebinding. This effect is even more pronounced in the case of Tf-trHb, where at least 40% of geminate recombination occurs in less than 300 ps. The occurrence of fast geminate rebinding and the differences in the CO rebinding kinetics registered for two apparently similar proteins highlight the strong influence played by the structural organization of the distal heme pocket and the interactions among the protein and the heme-ligand complex. Globin proteins are not the only example where such an effect is observed. Other systems where protein ligand interactions can have a strong influence on the photodynamics are found for instance in the rhodopsin family, where strong differences in the dynamics of retinal photoisomerization have been measured between visual pigments and microbial rhodopsin.[55] It is evident that a detailed understanding of such interactions is necessary in order to completely characterize the photodynamics of these systems. Regarding the two proteins analyzed in this study, further analysis on site directed mutants will allow an even more accurate characterization of the specific interactions of each of the residues present in the distal pocket with the ligand, which will eventually help to clarify the behavior of these proteins in their living environment.

ASSOCIATED CONTENT

Supporting Information

Baseline subtraction procedure for data at 2050−2150 cm^{-1}; EADS of time-resolved data in the free CO absorption region; influence of the baseline in the bleaching region; comparison between the kinetics at 2120 cm^{-1}; and the time dependence of the integrated area of the CO band. This material is available free of charge via the Internet at http://pubs.acs.org.

AUTHOR INFORMATION

Author Contributions

[¶]These two authors have equally contributed to this work

Notes

The authors declare no competing financial interest.

ACKNOWLEDGMENTS

The authors acknowledge the Italian 'Ministero dell'Istruzione dell'Università e della Ricerca' (PRIN 2008, 2008BFJ34R) and Istituto Pasteur Fondazione Cenci Bolognetti. A.L. and A.M. acknowledge the financial support of the Regione Toscana through the found POR FSE 2007-2013 obiettivo 2 asse IV, project EPHODS. The financial support of the Cassa di Risparmio di Firenze is also gratefully acknowledged.

REFERENCES

(1) Wittenberg, J. B.; Bolognesi, M.; Wittenberg, B. A.; Guertin, M. *J. Biol. Chem.* **2002**, *277* (2), 871−874.

(2) Wu, G.; Wainwright, L. M.; Poole, R. K., Microbial globins. In *Advances in Microbial Physiology*, Academic Press: 2003; Vol. *47*, pp 255−310.

(3) Feis, A.; Lapini, A.; Catacchio, B.; Brogioni, S.; Foggi, P.; Chiancone, E.; Boffi, A.; Smulevich, G. *Biochemistry* **2007**, *47* (3), 902−910.

(4) Guallar, V.; Lu, C.; Borrelli, K.; Egawa, T.; Yeh, S.-R. *J. Biol. Chem.* **2009**, *284* (5), 3106−3116.

(5) Ouellet, H.; Milani, M.; LaBarre, M.; Bolognesi, M.; Couture, M.; Guertin, M. *Biochemistry* **2007**, *46* (41), 11440−11450.

(6) Milani, M.; Pesce, A.; Nardini, M.; Ouellet, H.; Ouellet, Y.; Dewilde, S.; Bocedi, A.; Ascenzi, P.; Guertin, M.; Moens, L.; Friedman, J. M.; Wittenberg, J. B.; Bolognesi, M. *J. Inorg. Biochem.* **2005**, *99* (1), 97−109.

(7) Pesce, A.; Nardini, M.; Milani, M.; Bolognesi, M. *IUBMB Life* **2007**, *59* (8−9), 535−541.

(8) Bonamore, A.; Ilari, A.; Giangiacomo, L.; Bellelli, A.; Morea, V.; Boffi, A. *FEBS J.* **2005**, *272* (16), 4189−4201.
(9) Giangiacomo, L.; Ilari, A.; Boffi, A.; Morea, V.; Chiancone, E. *J. Biol. Chem.* **2005**, *280* (10), 9192−9202.
(10) Droghetti, E.; Nicoletti, F. P.; Bonamore, A.; Boechi, L.; Arroyo Manìfez, P.; Estrin, D. A.; Boffi, A.; Smulevich, G.; Feis, A. *Biochemistry* **2010**, *49* (49), 10394−10402.
(11) Yoshimura, H.; Yoshioka, S.; Kobayashi, K.; Ohta, T.; Uchida, T.; Kubo, M.; Kitagawa, T.; Aono, S. *Biochemistry* **2006**, *45* (27), 8301−8307.
(12) Frauenfelder, H.; McMahon, B. H.; Fenimore, P. W. *Proc. Natl. Acad. Sci.* **2003**, *100* (15), 8615−8617.
(13) Lim, M.; Jackson, T. A.; Anfinrud, P. A. *J. Chem. Phys.* **1995**, *102*, 4355−4366.
(14) Nuernberger, P.; Lee, K. F.; Bonvalet, A.; Bouzhir-Sima, L.; Lambry, J.-C.; Liebl, U.; Joffre, M.; Vos, M. H. *J. Am. Chem. Soc.* **2011**, *133* (43), 17110−17113.
(15) van Wilderen, L. J. G. W.; Key, J. M.; Van Stokkum, I. H. M.; van Grondelle, R.; Groot, M. L. *J. Phys. Chem. B* **2008**, *113* (11), 3292−3297.
(16) Kim, S.; Lim, M. *J. Am. Chem. Soc.* **2005**, *127* (16), 5786−5787.
(17) Lim, M.; Jackson, T. A.; Anfinrud, P. A. *Nat. Struct. Mol. Biol.* **1997**, *4* (3), 209−214.
(18) Nienhaus, K.; Dominici, P.; Astegno, A.; Abbruzzetti, S.; Viappiani, C.; Nienhaus, G. U. *Biochemistry* **2010**, *49* (35), 7448−7458.
(19) Polack, T.; Ogilvie, J. P.; Franzen, S.; Vos, M. H.; Joffre, M.; Martin, J. L.; Alexandrou, A. *Phys. Rev. Lett.* **2004**, *93* (1), 018102.
(20) Touron Touceda, P.; Mosquera Vazquez, S.; Lima, M.; Lapini, A.; Foggi, P.; Dei, A.; Righini, R. *Phys. Chem. Chem. Phys. 14* (2), 1038−1047.
(21) Afrawal, G. P.; Baldeck, P. L.; Alfano, R. R. *Phys. Rev. A* **1989**, *40*, 5063−5072.
(22) Hamm, P. *Chem. Phys.* **1995**, *200* (3), 415−429.
(23) Wynne, K.; Hochstrasser, R. M. *Chem. Phys.* **1995**, *193* (3), 211−236.
(24) Lian, T.; Kholodenko, Y.; Locke, B.; Hochstrasser, R. M. *J. Phys. Chem.* **1995**, *99* (19), 7272−7280.
(25) Lapini, A.; Mosquera Vázquez, S.; Tourón Touceda, P.; Lima, M. *J. Mol. Struct.* **2011**, *993* (1−3), 470−473.
(26) Hendler, R. W.; Shrager, R. I. *J. Biochem. Biophys. Methods* **1994**, *28* (1), 1−33.
(27) Henry, E. R. *Biophys. J.* **1997**, *72* (2), 652−673.
(28) Henry, E. R.; Hofrichter, J.; Ludwig Brand, M. L. J. Singular value decomposition: Application to analysis of experimental data. In *Methods Enzymolology*; Academic Press: San Diego, CA, 1992; Vol. *210*, pp 129−192.
(29) Dioumaev, A. K. *Biophys. Chem.* **1997**, *67*, 1−25.
(30) Bonneau, R.; Wirz, J.; Zuberbuhler, A. D. *Pure Appl. Chem.* **1997**, *69*, 979−992.
(31) Henry, E. R. *Biophys. J.* **1997**, *72*, 652−673.
(32) Franzen, S.; Kiger, L.; Poyart, C.; Martin, J. L. *Biophys. J.* **2001**, *80*, 2372−2385.
(33) van Stokkum, I. H. M.; Scherer, T.; Brouwer, A. M.; Verhoeven, J. W. *J. Phys. Chem.* **1994**, *98* (3), 852−866.
(34) van Stokkum, I. H. M.; Larsen, D. S.; van Grondelle, R. *Biochim. Biophys. Acta* **2004**, *1657*, 82.
(35) Satzger, H.; Zinth, W. *Chem. Phys.* **2003**, *295* (3), 287−295.
(36) Neumann, K.; Verhoefen, M.-K.; Weber, I.; Glaubitz, C.; Wachtveitl, J. *Biophys. J.* **2008**, *94* (12), 4796−4807.
(37) Mullen, K. M.; van Stokkum, I. H. M. *J. Stat. Software* **2007**, *18* (1), 1−5.
(38) Mullen, K. M.; van Stokkum, I. H. M. *J. Stat. Software* **2007**, *18* (3), 1−46.
(39) Cador, O.; Chabre, F.; Dei, A.; Sangregorio, C.; Slageren, J. V.; Vaz, M. G. F. *Inorg. Chem.* **2003**, *42* (20), 6432−6440.
(40) Snellenburg, J. J.; Laptenok, S. P.; Seger, R.; Mullen, K. M.; van Stokkum, I. H. M. Glotaran: A Java-Based Graphical User Interface for the R Package TIMP; *Journal of Statistical Software*, *49* (3), 1−22, http://www.jstatsoft.org/v49/i03/.
(41) Lim, M.; Jackson, T. A.; Anfinrud, P. A. *J. Am. Chem. Soc.* **2004**, *126* (25), 7946−7957.
(42) Moore, J. N.; Hansen, P. A.; Hochstrasser, R. M. *Proc. Natl. Acad. Sci.* **1988**, *85* (14), 5062−5066.
(43) Anfinrud, P. A.; Han, C.; Hochstrasser, R. M. *Proc. Natl. Acad. Sci.* **1989**, *86* (21), 8387−8391.
(44) Lim, M.; Jackson, T. A.; Anfinrud, P. A. *J. Phys. Chem.* **1996**, *100* (29), 12043−12051.
(45) Hush, N. S.; Williams, M. L. *J. Mol. Spectrosc.* **1974**, *50*, 349−368.
(46) Sagnella, D. E.; Straub, J. E.; Jackson, T. A.; Lim, M.; Anfinrud, P. A. *Proc. Natl. Acad. Sci.* **1999**, *96* (25), 14324−14329.
(47) Nuernberger, P.; Lee, K. F.; Bonvalet, A.; Vos, M. H.; Joffre, M. *J. Phys. Chem. Lett.* **2010**, *1* (14), 2077−2081.
(48) Jasaitis, A.; Hola, K.; Bouzhir-Sima, L.; Lambry, J.-C.; Balland, V.; Vos, M. H.; Liebl, U. *Biochemistry* **2006**, *45* (19), 6018−6026.
(49) Boechi, L.; Mañez, P. A.; Luque, F. J.; Marti, M. A.; Estrin, D. A. *Proteins: Struct., Funct., Bioinform.* **2010**, *78* (4), 962−970.
(50) Grogan, T. G.; Bag, N.; Traylor, T. G.; Magde, D. *J. Phys. Chem.* **1994**, *98* (51), 13791−13796.
(51) Jasaitis, A.; Ouellet, H.; Lambry, J.-C.; Martin, J.-L.; Friedman, J. M.; Guertin, M.; Vos, M. H. *Chem. Phys.* **2012**, *396*, 10−16.
(52) Kim, J.; Park, J.; Lee, T.; Lim, M. *J. Phys. Chem. B* **2008**, *113* (1), 260−266.
(53) Lim, M.; Jackson, T. A.; Anfinrud, P. A. *J. Biol. Inorg. Chem.* **1997**, *2*, 531−536.
(54) Silkstone, G.; Jasaitis, A.; Vos, M. H.; Wilson, M. T. *Dalton Trans.* **2005**, *21*, 3489−3494.
(55) Wand, A.; Rozin, R.; Eliash, T.; Jung, K.-H.; Sheves, M.; Ruhman, S. *J. Am. Chem. Soc.* **2011**, *133* (51), 20922−20932.